

Received 13 December 2022, accepted 4 January 2023, date of publication 5 January 2023,  
date of current version 10 January 2023.

Digital Object Identifier 10.1109/ACCESS.2023.3234864

## RESEARCH ARTICLE

# Model-Free Controller Design for Nonlinear Underactuated Systems With Uncertainties and Disturbances by Using Extended State Observer Based Chattering-Free Sliding Mode Control

ÜMIT ÖNEN 

Department of Mechatronics Engineering, Necmettin Erbakan University, 42100 Konya, Turkey


e-mail: uonen@erbakan.edu.tr

**ABSTRACT** Most of the control strategies require a mathematical model or reasonable knowledge that is difficult to obtain for complex systems. Model-free control is a good alternative to avoid the difficulties and complex modeling procedures, especially if the knowledge about the system is insufficient. This paper presents a new control scheme completely independent of the system model. The proposed scheme combines sliding mode control (SMC) with intelligent proportional integral derivative (iPID) control based on a local model and extended state observer (ESO). Although the iPID control makes the proposed method model-free, it cannot guarantee that the tracking errors converge to zero asymptotically except the system is in a steady-state regime. Therefore, the SMC is added to the control scheme to ensure the convergence by minimizing the estimation errors of the observer. The proposed iPIDSMC controller is tested in the presence of different parameter variations and external disturbances on an inverted pendulum - cart (IPC), which is a highly unstable underactuated system with nonlinear coupled dynamics. The proposed controller is compared with the PID, iPID and Hierarchical Sliding Mode Control (HSMC) for a clearer evaluation. Simulation results showed that the proposed controller is extremely insensitive to parameter variations, matched and mismatched disturbances and the control signal of the proposed method is chattering-free, even though it is based on a discontinuous control action.

**INDEX TERMS** Extended state observer, external disturbance, intelligent PID, model-free control, robust control, sliding mode control, uncertainties, underactuated system.

## I. INTRODUCTION

Underactuated systems are used in many applications in different fields due to their advantages of less complexity, low cost and energy consumption. But, using a lower number of actuators than the degree of freedom causes dynamic coupling between the states and instability in the system response. Inverted pendulums (IPs) are one of the most known underactuated systems. Their nonlinear, coupled and extremely unstable dynamic characteristics cause the control of inverted pendulums a challenging task and make them

The associate editor coordinating the review of this manuscript and approving it for publication was Mou Chen .

an excellent tool for testing the performances of control techniques. However, most of the electromechanical systems used in practical applications have parameter uncertainties and external disturbances because of the mass variations, actuator saturation, external forces, damping, friction, sensor noises, etc. Therefore, proposed controllers should be robust and insensitive to the system uncertainties and external disturbances as well as provide a fast system response and good tracking performance.

Various control techniques have been proposed for the stability control of IP systems. Linear control methods such as Proportional Integral Derivative (PID) [1], [3], [4], Fractional Order PID [2] and Linear Quadratic Regulator (LQR) [1], [4]

have been used in the control of IPs. The linear controllers are easy to implement and very effective in control of certain systems but use of linearized model may cause to instability and poor closed-loop behavior since it cannot fully represent the dynamics of nonlinear systems. Furthermore, the linear controllers are very sensitive to the parameter uncertainties and external disturbances in general. The performance of the linear controllers directly depends on the controller parameters and finding optimum parameters for complex nonlinear systems is quite a difficult task. Some researchers have used meta-heuristic algorithms such as Adaptive Swarm Learning Process [3], Genetic Algorithm [4], Particle Swarm Optimization [4], Artificial Bee Colony [4] to find optimal controller gains and weighting matrices. However, a set of controller parameters is only effective under limited conditions and the validity region is small. Some researchers have combined PID control with fuzzy logic [5], neural networks [6] and Lyapunov stability theory [7] to extend the validity region and increase the robustness. Model predictive control (MPC) that requires an accurate system model, has been used for the stability control of IPs [8], [9], [10]. The major disadvantage of the MPC control is the difficulty of obtaining an accurate model for complex nonlinear systems. Optimal control techniques based on the minimization of the cost functional such as Linear Quadratic Gaussian (LQG),  $H_\infty$  and  $H_2$  has been used in the control of IPs [11]. But these controllers are only optimal with respect to the defined cost function. Both MPC and Optimal controllers can provide robustness against the model uncertainties and the disturbances if a sufficiently accurate system model can be obtained. Intelligent control techniques such as Neural Networks (NN) [12], [13] and Fuzzy Logic (FLC) [14], [15], [16] have been frequently used in the control of IP systems due to less model dependency and low computational requirements. But, the NN requires a large experimental dataset and the FLC requires knowledge of the system's behavior and a complex rule base for higher order systems. Nonlinear control techniques such as Backstepping [17] and Sliding mode control (SMC) [18], [19], [20], [21], [22] have been frequently used in the control of nonlinear systems with both external and internal disturbances because of their superior stability and robustness features. The major disadvantages of the SMC are the difficulties encountered in its application to underactuated systems and the chattering phenomenon, which causes the instability and damage in practical systems. Furthermore, the most of the existing traditional SMC approaches are insensitive only to matched disturbances and cannot attenuate mismatched disturbances effectively. Various SMC methods such as Terminal SMC [18], [19], Super-Twisting SMC [20], Disturbance observer based integral SMC [21], Fractional order SMC [22] have been proposed to overcome these problems. Some recent advances on SMC for the systems subject to uncertainty and disturbance are summarized in [23]. Active Disturbance Rejection Control (ADRC) consisting of a tracking differentiator, a state observer and an output feedback controller is

an alternative control strategy used in the stability control of pendulum systems [24], [25]. The total disturbance, including the internal and external disturbances, is estimated using the online state observer and decoupled from the system by defining it as a new virtual state. This yields to obtain a simplified system model since it compensates for the negative effects of modeling uncertainties in real time. Output Feedback Control [26] and Event Triggered control [27], [28] are the other methods proposed for the control of systems affected by model uncertainties and disturbances.

Most of the aforementioned control strategies require a system model or reasonably precise information about the system. Based on the amount of physical and mathematical information of the system, model-based controllers have provided a successful control performance for many systems. However, model-free control techniques can be used as an effective alternative to avoid difficult and complex modeling procedures or where there is insufficient knowledge of the system. The model-free control techniques estimate the dynamic behavior of the system without the requirement of a mathematical model or any knowledge other than input-output information and generate the appropriate control inputs for upcoming time steps. Intelligent PID (iPID) presented in [29], [30], and [31] is one of the most known model-free control techniques. iPID control of inertia wheel inverted pendulum and two-wheeled inverted pendulum is presented in [32] and [33] respectively. Model-free control of rotary pendulum based on classical PID and SMC is presented in [34]. Backstepping model-free control of rotary inverted pendulum is proposed in [35] and model-free control based on Legendre polynomials is presented in [36]. Some intelligent techniques have been used for model-free control. Model-free control of a single inverted pendulum based on reinforcement learning is presented in [37], model-free adaptive control of rotary inverted pendulum based on long-term predictor learning is proposed in [38] and model-free adaptive output recurrent cerebellar model articulation control of wheeled inverted pendulum is presented in [39]. All of these studies have shown remarkable success of model-free control techniques, especially on systems having model uncertainties and external disturbance.

In this study, the design procedure of a novel model-free control scheme based on the combination of iPID and SMC control is presented. First, the iPID controller, consisting of a local model and an extended state observer (ESO) is designed. Then, the SMC is added to the control scheme to minimize the estimation errors of the ESO and ensure the convergence of tracking errors to zero in finite time. Stability analysis of the proposed controller based on Lyapunov theory is given. The proposed control scheme is tested on a highly unstable, nonlinear underactuated system in the presence of different parameter variations and external disturbances. The performance of the proposed controller is compared with PID, iPID and HSMC controllers for a clearer evaluation. The simulation results showed that the proposed controller is extremely successful in terms of response speed, robustness

and disturbance rejection ability. The main contributions of the paper can be summarized as follows:

- Most of the control studies in the literature require a linear/nonlinear system model or at least sufficient information about the system. However, in practical applications, modeling of complex systems is a very difficult task and it is almost impossible to obtain a precise system model after many assumptions and linearization. In this study design procedure of a novel model-free control methods is given. The proposed controller does not require a system model or any information about the system other than input-output information. Therefore, it can be easily applied to any complex system without complex modeling procedure.
- Most of the model-independent control methods available in the literature are learning-based methods. These methods require complex network structures and rule tables, as well as they have a large number of parameters to be set and a heavy computational load. The proposed control method is based on an extremely simple local model compared to learning-based control methods. This local model uses input-output information to constantly update itself in a short time horizon and requires much less computation.
- In addition to design procedure, the stability of the proposed control scheme is proved based on Lyapunov approach. Also, it is proven by the various simulation studies that the proposed control scheme is completely insensitive to parameter changes and it has a superior disturbance rejection ability against the disturbances. In most of the studies in the literature, model uncertainties, parameter variations and matching disturbances were taken into account when evaluating the controller performance. The matched disturbances always get involved the system via the same channel with the control input. On the other hand, mismatched disturbances extensively exist in the real world. Different from the matching disturbances, these disturbances act on the system via the different channel from the control input and dealing with them is more challenging. In this study, a comprehensive simulation study is carried out in which mismatched disturbances are taken into account in addition to parameter changes and matched disturbances. The simulation results showed that the proposed controller is extremely effective, especially against the mismatched disturbances.
- The proposed control scheme is chattering-free even though it is based on a discontinuous control action. This proves the proposed control scheme generates an ideal sliding mode by successfully eliminating the effect of uncertainties and disturbances that cause chattering.

## II. PRELIMINARIES

### A. PROBLEM STATEMENT

In real systems, unavoidable model uncertainties and disturbances due to modeling simplifications, mass variations,

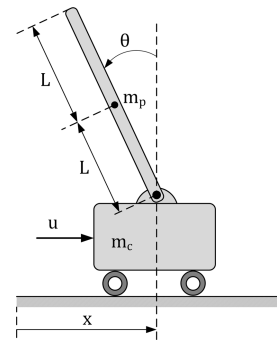


FIGURE 1. Schematic view of the inverted pendulum - cart system.

actuator saturation, damping, friction, sensor noise, etc. make the control problem much more difficult. One of the best ways to deal with this problem is to design a controller that does not require a system model.

An inverted pendulum-cart (IPC) system, one of the best known examples of under-actuated systems, is used to evaluate the performance of the model-free controller proposed in this study. Because, it is an inherently highly unstable system with nonlinear coupled dynamics in addition to being extremely sensitive to uncertainties and disturbances. In addition to these difficulties, since the IPC system is an under-actuated system, two different state variables have to be controlled with a single control signal.

In this study, the position and stability control of the IPC system is considered. The aim of the control is to bring the cart to the desired position in the shortest time while keeping the pendulum stable in the vertical position, in the presence of all model uncertainties and disturbances.

### B. SYSTEM DESCRIPTION

The schematic view of the IPC system considered in this study is given in 1. The equations of motion of the system can be derived by Euler-Lagrange formulation as;

$$\ddot{x}(t) = (-h_1^2 g \cos(\theta) \sin(\theta) - h_1 h_3 \sin(\theta) \dot{\theta}^2 + h_3 u(t)) / (h_2 h_3 - h_1^2 \cos^2(\theta)) \quad (1)$$

$$\ddot{\theta}(t) = (-h_1^2 \cos(\theta) \sin(\theta) \dot{\theta}^2 - h_1 h_2 g \sin(\theta) + h_1 \cos(\theta) u(t)) / (h_2 h_3 - h_1^2 \cos^2(\theta)) \quad (2)$$

where  $h_1 = m_p L$ ,  $h_2 = m_c + m_p$ ,  $h_3 = I_p + m_p L^2$ . Here,  $m_c$  and  $m_p$  denotes the cart mass and the pendulum mass, respectively,  $I_p$  denotes the moment of inertia of the pendulum with respect to its axis on the cart.  $L$  is the half-length of the pendulum,  $x(t)$  is the cart position and  $\theta(t)$  is the pendulum angle.  $u(t)$  is the control force applied to the cart in  $x$ -direction.

Note that the dynamic model of the system is obtained only for use in simulation studies and is not considered in the controller design.

### III. iPID CONTROLLER DESIGN

i-PID controller is a PID controller where the unknown parts of the system are taken into account without any

modelling procedure [29]. It is based on a local model which is continuously updated via input-output information of the system. So, the unknown ‘complex’ mathematical model is replaced by an ultra-local model. The main advantages of the i-PID controller can be summarized as: (i) It does not require a system model or any knowledge about the system. So, it can be easily implemented to every kind of complex system which might be highly nonlinear and/or time-varying. (ii) Besides having all the advantages of PID control, the tuning of the gains is straight forward since the unknown parts of the model is eliminated. (iii). Unlike many other model-free control methods, i-PID control does not need a large data set and complex algorithms to modelling system behaviors. This feature makes it different from “black-box” models, which is valid within a certain operating range. For a single input-single output (SISO) system, the local model has been defined in [31] as follows:

$$y^{(v)}(t) = \varphi(t) + \alpha u(t) \tag{3}$$

where  $y(t)$  is the output,  $u(t)$  is the control signal,  $v$  is the derivation order selected as 1 or 2,  $\alpha$  is a non-physical constant parameter which can be chosen such that  $\alpha u$  and  $y^{(v)}$  are of the same magnitude.  $\varphi(t)$  is a function, which is the sum of unknown dynamics and disturbances of the system. The numerical value of  $\varphi(t)$  is determined at each time interval from input-output behavior of the system. The system can be divided into two subsystems as cart and pendulum. Based on the iPID theory, the local models of the two subsystems can be defined as follows.

$$\ddot{x}(t) = \varphi_x(t) + \alpha_x u_x(t) \tag{4}$$

$$\ddot{\theta}(t) = \varphi_\theta(t) + \alpha_\theta u_\theta(t) \tag{5}$$

Two different iPID controllers are designed for the two subsystems as shown in Fig. 2. The first controller is responsible for the cart position  $x(t)$  while the second one is responsible for the pendulum angle  $\theta(t)$ . The control input of the each iPID controller can be defined as;

$$u_x(t) = \frac{1}{\alpha_x} \left( K_{p1} e_x(t) + K_{d1} \dot{e}_x(t) + K_{i1} \int e_x(t) + \ddot{x}_r(t) - \hat{\varphi}_x(t) \right) \tag{6}$$

$$u_\theta(t) = \frac{1}{\alpha_\theta} \left( K_{p2} e_\theta(t) + K_{d2} \dot{e}_\theta(t) + K_{i2} \int e_\theta(t) + \ddot{\theta}_r(t) - \hat{\varphi}_\theta(t) \right) \tag{7}$$

where  $K_{p1}, K_{d1}, K_{i1}$  are the gains of the first PID controller,  $K_{p2}, K_{d2}, K_{i2}$  are the gains of the second PID controller,  $\hat{\varphi}_x(t)$  and  $\hat{\varphi}_\theta(t)$  are the estimated values of  $\varphi_x(t)$  and  $\varphi_\theta(t)$  respectively,  $\ddot{x}_r(t)$  and  $\ddot{\theta}_r(t)$  are the second derivatives of the reference trajectories of the state variables  $x(t)$  and  $\theta(t)$ . The state errors are defined as  $e_x(t) = x_r(t) - x(t)$  and  $e_\theta(t) = \theta_r(t) - \theta(t)$ .

TABLE 1. Characteristics of the desired step response.

| Parameter               | Value |
|-------------------------|-------|
| Step Time (seconds)     | 0     |
| Rise Time (seconds)     | 1.28  |
| Settling Time (seconds) | 2.6   |
| Initial Value           | 0     |
| Final Value             | 0.5   |
| % Overshoot             | 1.45  |
| % Rise                  | 75    |
| % Settling              | 1.4   |

Substituting (6) and (7) in (4) and (5) respectively, error dynamics of the subsystems are obtained as follows.

$$\ddot{e}_x(t) + \varphi_x(t) - \hat{\varphi}_x(t) + K_{p1} e_x(t) + K_{d1} \dot{e}_x(t) + K_{i1} \int e_x(t) = 0 \tag{8}$$

$$\ddot{e}_\theta(t) + \varphi_\theta(t) - \hat{\varphi}_\theta(t) + K_{p2} e_\theta(t) + K_{d2} \dot{e}_\theta(t) + K_{i2} \int e_\theta(t) = 0 \tag{9}$$

Estimation errors can be defined as  $\tilde{\varphi}_x(t) = \varphi_x(t) - \hat{\varphi}_x(t)$  and  $\tilde{\varphi}_\theta(t) = \varphi_\theta(t) - \hat{\varphi}_\theta(t)$ . It is obvious that the steady errors of the closed loop system depend on the controller gains  $K_{p1}, K_{d1}, K_{i1}, K_{p2}, K_{d2}, K_{i2}$  and the estimation errors  $\tilde{\varphi}_x(t)$  and  $\tilde{\varphi}_\theta(t)$ .

Assumption 1: The unknown lumped disturbances  $\varphi_x(t)$  and  $\varphi_\theta(t)$  are continuous and their derivatives  $\dot{\varphi}_x$  and  $\dot{\varphi}_\theta$  satisfy  $\|\dot{\varphi}_x(t)\| \leq \gamma_x$  and  $\|\dot{\varphi}_\theta(t)\| \leq \gamma_\theta$  where  $\gamma_x$  and  $\gamma_\theta$  are unknown positive constants.

An Extended State Observer is designed to estimate  $\tilde{\varphi}_x(t)$  and  $\tilde{\varphi}_\theta(t)$  values. In addition, the controller gains are optimized using “Simplex Search” algorithm. The gains  $K_{p1}, K_{d1}$  and  $K_{i1}$  are optimized according to the desired step response of the cart position  $x(t)$  whereas the gains  $K_{p2}, K_{d2}$  and  $K_{i2}$  are optimized to keep the pendulum angle  $\theta(t)$  within a very limited range close to zero. Desired pendulum angle range is selected as  $\pm 0.01$  rad and the characteristics of the desired step response are given in Table 1.

Besides having a simple structure, the ESO can efficiently estimates both the system states and the total disturbance, which is sum of the model uncertainties and external disturbances. It only requires input-output information of the system and can be expanded corresponding to the number of system states. The subsystems in (4) and (5) can be written in state-space form as follows by defining  $\varphi_x(t)$  and  $\varphi_\theta(t)$  as additional state variables such as  $x_3(t) = \varphi_x(t)$  and  $\theta_3(t) = \varphi_\theta(t)$ .

$$\begin{cases} \dot{x}_1(t) = x_2(t) \\ \dot{x}_2(t) = \varphi_x(t) + \alpha_x u_x(t) \\ \dot{x}_3(t) = \dot{\varphi}_x(t) \end{cases} \tag{10}$$

$$\begin{cases} \dot{\theta}_1(t) = \theta_2(t) \\ \dot{\theta}_2(t) = \varphi_\theta(t) + \alpha_\theta u_\theta(t) \\ \dot{\theta}_3(t) = \dot{\varphi}_\theta(t) \end{cases} \tag{11}$$

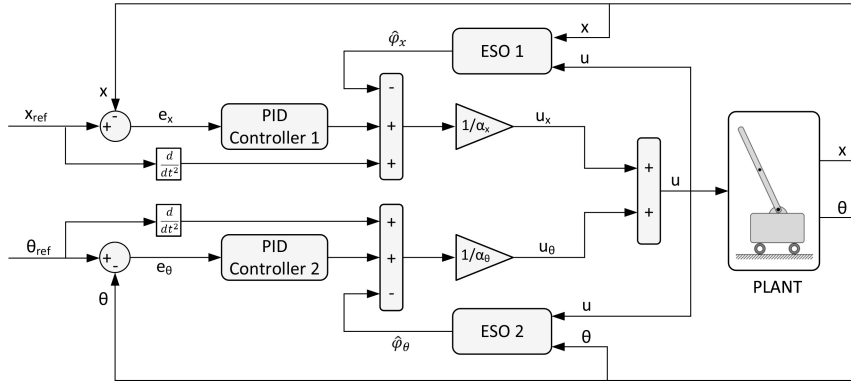


FIGURE 2. iPID control scheme of the inverted pendulum system.

The extended state observers for the subsystems given in (10) and (11) can be designed as

$$\begin{cases} \dot{\hat{x}}_1(t) = \hat{x}_2(t) + \beta_{x1}\tilde{x}_1(t) \\ \dot{\hat{x}}_2(t) = \hat{x}_3(t) + \beta_{x2}\tilde{x}_1(t) + \alpha_x u_x(t) \\ \dot{\hat{x}}_3(t) = \beta_{x3}\tilde{x}_1(t) \end{cases} \quad (12)$$

$$\begin{cases} \dot{\hat{\theta}}_1(t) = \hat{\theta}_2(t) + \beta_{\theta1}\tilde{\theta}_1(t) \\ \dot{\hat{\theta}}_2(t) = \hat{\theta}_3(t) + \beta_{\theta2}\tilde{\theta}_1(t) + \alpha_\theta u_\theta(t) \\ \dot{\hat{\theta}}_3(t) = \beta_{\theta3}\tilde{\theta}_1(t) \end{cases} \quad (13)$$

where  $\hat{x}_1(t), \hat{x}_2(t), \hat{\theta}_1(t), \hat{\theta}_2(t)$  are the estimations of  $x_1(t), x_2(t), \theta_1(t), \theta_2(t)$  and  $\hat{x}_3(t), \hat{\theta}_3(t)$  are the estimations of  $\varphi_x(t)$  and  $\varphi_\theta(t)$  respectively.  $\beta_{x1}, \beta_{x2}, \beta_{x3}, \beta_{\theta1}, \beta_{\theta2}, \beta_{\theta3}$  are the observer gains,  $\tilde{x}_1(t) = x_1(t) - \hat{x}_1(t)$  and  $\tilde{\theta}_1(t) = \theta_1(t) - \hat{\theta}_1(t)$  are the estimation errors of the  $x_1(t)$  and  $\theta_1(t)$  respectively. From (8)-(13), the estimation errors of the observers can be defined as

$$\begin{cases} \dot{\tilde{x}}_1(t) = \tilde{x}_2(t) - \beta_{x1}\tilde{x}_1(t) \\ \dot{\tilde{x}}_2(t) = \tilde{x}_3(t) - \beta_{x2}\tilde{x}_1(t) \\ \dot{\tilde{x}}_3(t) = \dot{\varphi}_x(t) - \beta_{x3}\tilde{x}_1(t) \end{cases} \quad (14)$$

$$\begin{cases} \dot{\tilde{\theta}}_1(t) = \tilde{\theta}_2(t) - \beta_{\theta1}\tilde{\theta}_1(t) \\ \dot{\tilde{\theta}}_2(t) = \tilde{\theta}_3(t) - \beta_{\theta2}\tilde{\theta}_1(t) \\ \dot{\tilde{\theta}}_3(t) = \dot{\varphi}_\theta(t) - \beta_{\theta3}\tilde{\theta}_1(t) \end{cases} \quad (15)$$

The state errors of the observers can be defined as  $\tilde{X} = [\tilde{x}_1, \tilde{x}_2, \tilde{x}_3]^T$  and  $\tilde{\theta} = [\tilde{\theta}_1, \tilde{\theta}_2, \tilde{\theta}_3]^T$ . Now, the overall estimation error dynamics for the subsystems in (4) and (5) can be written in the following form.

$$\dot{\tilde{X}} = A_x \tilde{X} + B_x \quad (16)$$

$$A_x = \begin{bmatrix} -\beta_{x1} & 1 & 0 \\ -\beta_{x2} & 0 & 1 \\ -\beta_{x3} & 0 & 0 \end{bmatrix}, B_x = \begin{bmatrix} 0 \\ 0 \\ \dot{\varphi}_x \end{bmatrix} \quad (17)$$

and

$$\dot{\tilde{\theta}} = A_\theta \tilde{\theta} + B_\theta \quad (18)$$

$$A_\theta = \begin{bmatrix} -\beta_{\theta1} & 1 & 0 \\ -\beta_{\theta2} & 0 & 1 \\ -\beta_{\theta3} & 0 & 0 \end{bmatrix}, B_\theta = \begin{bmatrix} 0 \\ 0 \\ \dot{\varphi}_\theta \end{bmatrix} \quad (19)$$

From (16) and (17), it is obvious that  $A_x$  is a Hurwitz matrix under the condition that  $\beta_{xi} > 0, i = 1..3$ , so there exists a positive definite matrix  $P_x$  such that

$$A_x^T P_x + P_x A_x = -Q_x \quad (20)$$

for any given positive definite matrix  $Q_x$ . Defining a Lyapunov candidate

$$\dot{V}(\tilde{X}) = \tilde{X}^T P_x \tilde{X} \quad (21)$$

and evaluating  $\dot{V}(\tilde{X})$  along (21)

$$\begin{aligned} \dot{V}(\tilde{X}) &= \dot{\tilde{X}}^T P_x \tilde{X} + \tilde{X}^T P_x \dot{\tilde{X}} \\ &= (A_x \tilde{X} + B_x)^T P_x \tilde{X} + \tilde{X}^T P_x (A_x \tilde{X} + B_x) \\ &= \tilde{X}^T A_x^T P_x \tilde{X} + \tilde{X}^T P_x A_x \tilde{X} + 2B_x^T P_x \tilde{X} \\ &= -\tilde{X}^T Q_x \tilde{X} + 2B_x^T P_x \tilde{X} \\ &\leq -\lambda_{\min}(Q_x) \|\tilde{X}\|^2 + 2\gamma_x \|P_x\| \|\tilde{X}\| \\ &= \|\tilde{X}\| (\lambda_{\min}(Q_x) \|\tilde{X}\| - 2\lambda_x \|P_x\|) \end{aligned} \quad (22)$$

Therefore, the norm of the estimation error  $\tilde{X}$  is bounded by

$$\|\tilde{X}\| \leq \frac{2\gamma_x \|P_x\|}{\lambda_{\min}(Q_x)} \quad (23)$$

within finite time where  $\lambda_{\min}(\cdot)$  is the smallest eigenvalue of a matrix. If the same process is applied to the second subsystem, whose error dynamics is given in (18) and (19), it can be seen that norm of the estimation error  $\tilde{\theta}$  is bounded within finite time by

$$\|\tilde{\theta}\| \leq \frac{2\gamma_\theta \|P_\theta\|}{\lambda_{\min}(Q_\theta)} \quad (24)$$

Lemma 1: [40] Given a differentiable continuous function  $\Psi(t), \forall t \in [t_0, t_1]$  satisfying  $\delta_1 \leq \|\Psi(t)\| \leq \delta_2$  with the positive constants  $\delta_1$  and  $\delta_2$ . Its derivative  $\dot{\Psi}(t)$  is also bounded according to ‘‘Mean Value Theorem’’. Therefore, the estimation errors of the lumped disturbances  $\varphi_x(t)$  and  $\varphi_\theta(t)$  are bounded.

Assumption 2: For  $\forall t \in R^+$ , the unknown lumped disturbances  $\varphi_x(t)$  and  $\varphi_\theta(t)$  of the subsystems are bounded. That is to say there exists positive constants that the inequalities  $\|\tilde{\varphi}_x\| \leq \varphi_{xup}$  and  $\|\tilde{\varphi}_\theta\| \leq \varphi_{\theta up}$  are satisfied.

The observer gains  $\beta_{x1}, \beta_{x2}, \beta_{x3}, \beta_{\theta1}, \beta_{\theta2}, \beta_{\theta3}$  can be computed from the characteristic polynomial of the ESO. The observer pole  $\omega_{ESO}$  is usually placed 3 - 10 times to the left of the closed loop pole  $\omega_C$  to ensure that the observer dynamics are fast enough. The respective solutions for the observer gains are as follows.

$$\begin{cases} \beta_{x1} = \beta_{\theta1} = 3\omega_{ESO}, \\ \beta_{x2} = \beta_{\theta2} = 3\omega_{ESO}^2, \\ \beta_{x3} = \beta_{\theta3} = 3\omega_{ESO}^3 \\ \omega_{ESO} = (3 - 10)\omega_C \end{cases} \quad (25)$$

It should be noted that the estimation error of the ESO monotonically decreases with increasing observer bandwidth in the absence of an accurate system model.

#### IV. IPIDSMC CONTROLLER DESIGN

The effectiveness of the control scheme depends on the success of the observer. As the estimation error increases, the control performance will decrease. Therefore, a SMC controller has been added to control scheme in order to minimize the observer errors. The proposed iPIDSMC control scheme is shown in Fig. 3. A separate SMC controller was designed for each subsystem and added to the corresponding iPID controller.

SMC control law consists of two parts as equivalent control and switching control. Equivalent control drives the system states to the sliding surface and switching control keeps the system states on the sliding surface. The total control input of the SMC is defined as;

$$u^s(t) = u^{eq}(t) + u^{sw}(t) \quad (26)$$

where  $u^{eq}(t)$  denotes the equivalent control signal and  $u^{sw}(t)$  denotes the switching control. Now the control inputs for the subsystems are written as follows.

$$u_x(t) = \frac{1}{\alpha_x} \left( K_{p1}e_x(t) + K_{d1}\dot{e}_x(t) + K_{i1} \int e_x(t) + \ddot{x}_r(t) - \hat{\varphi}_x(t) \right) + u_x^s(t) \quad (27)$$

$$u_\theta(t) = \frac{1}{\alpha_\theta} \left( K_{p2}e_\theta(t) + K_{d2}\dot{e}_\theta(t) + K_{i2} \int e_\theta(t) + \ddot{\theta}_r(t) - \hat{\varphi}_\theta(t) \right) + u_\theta^s(t) \quad (28)$$

Substituting (6) and (7) into (4) and (5) respectively, the error dynamics of the subsystems are obtained as follows.

$$\begin{aligned} \ddot{e}_x(t) + \tilde{\varphi}_x(t) + K_{p1}e_x(t) + K_{d1}\dot{e}_x(t) \\ + K_{i1} \int e_x(t) + \alpha_x u_x^s(t) = 0 \end{aligned} \quad (29)$$

$$\begin{aligned} \ddot{e}_\theta(t) + \tilde{\varphi}_\theta(t) + K_{p2}e_\theta(t) + K_{d2}\dot{e}_\theta(t) \\ + K_{i2} \int e_\theta(t) + \alpha_\theta u_\theta^s(t) = 0 \end{aligned} \quad (30)$$

Sliding surfaces of the cart and pendulum subsystems can be defined as,

$$s_x(t) = c_1 e_x(t) + \dot{e}_x(t) \quad (31)$$

$$s_\theta(t) = c_2 e_\theta(t) + \dot{e}_\theta(t) \quad (32)$$

where  $c_1$  and  $c_2$  are positive constants. Derivatives of (31) and (32) are as follows.

$$\dot{s}_x(t) = c_1 \dot{e}_x(t) + \ddot{e}_x(t) \quad (33)$$

$$\dot{s}_\theta(t) = c_2 \dot{e}_\theta(t) + \ddot{e}_\theta(t) \quad (34)$$

If we subtract  $\ddot{e}_x(t)$  in (29) and  $\ddot{e}_\theta(t)$  in (30) and substitute them into (33) and (34) respectively and then equate to zero, the equivalent control laws can be obtained as follows.

$$\begin{aligned} u_x^{eq}(t) = \frac{1}{\alpha_x} \left( c_1 \dot{e}_x(t) - \varphi_{xup} - K_{p1}e_x(t) \right. \\ \left. - K_{d1}\dot{e}_x(t) - K_{i1} \int e_x(t) \right) \end{aligned} \quad (35)$$

$$\begin{aligned} u_\theta^{eq}(t) = \frac{1}{\alpha_\theta} \left( c_2 \dot{e}_\theta(t) - \varphi_{\theta up} - K_{p2}e_\theta(t) \right. \\ \left. - K_{d2}\dot{e}_\theta(t) - K_{i2} \int e_\theta(t) \right) \end{aligned} \quad (36)$$

In order to satisfy the reaching conditions, switching control laws are selected as,

$$u_x^{sw}(t) = \frac{1}{\alpha_x} \left( \kappa_x s_x(t) + \eta_x \text{sgn}(s_x(t)) \right) \quad (37)$$

$$u_\theta^{sw}(t) = \frac{1}{\alpha_\theta} \left( \kappa_\theta s_\theta(t) + \eta_\theta \text{sgn}(s_\theta(t)) \right) \quad (38)$$

where  $\kappa_x, \kappa_\theta, \eta_x$  and  $\eta_\theta$  are positive constants.

The total SMC input for the cart subsystem can be obtained by substituting (37) and (38) in (26) as follows.

$$\begin{aligned} u_x^s(t) = \frac{1}{\alpha_x} \left( c_1 \dot{e}_x(t) \varphi_{xup} - K_{p1}e_x(t) - K_{d1}\dot{e}_x(t) \right. \\ \left. - K_{i1} \int e_x(t) + \kappa_x s_x(t) + \eta_x \text{sgn}(s_x(t)) \right) \end{aligned} \quad (39)$$

Similarly, total SMC input for the pendulum subsystem is obtained as

$$\begin{aligned} u_\theta^s(t) = \frac{1}{\alpha_\theta} \left( c_2 \dot{e}_\theta(t) - \varphi_{\theta up} - K_{p2}e_\theta(t) - K_{d2}\dot{e}_\theta(t) \right. \\ \left. - K_{i2} \int e_\theta(t) + \kappa_\theta s_\theta(t) + \eta_\theta \text{sgn}(s_\theta(t)) \right) \end{aligned} \quad (40)$$

Substituting (39) into (27) and (40) into (28), the total control inputs of the cart and pendulum subsystems are obtained as

$$\begin{aligned} u_x(t) = \frac{1}{\alpha_x} \left( \ddot{x}_r(t) - \hat{\varphi}_x(t) - \varphi_{xup} + c_1 \dot{e}_x(t) \right. \\ \left. + \kappa_x s_x(t) + \eta_x \text{sgn}(s_x(t)) \right) \end{aligned} \quad (41)$$

$$\begin{aligned} u_\theta(t) = \frac{1}{\alpha_\theta} \left( \ddot{\theta}_r(t) - \hat{\varphi}_\theta(t) - \varphi_{\theta up} + c_2 \dot{e}_\theta(t) \right. \\ \left. + \kappa_\theta s_\theta(t) + \eta_\theta \text{sgn}(s_\theta(t)) \right) \end{aligned} \quad (42)$$

Finally, the total control input of the system can be as follows.

$$u(t) = u_x(t) + u_\theta(t)$$

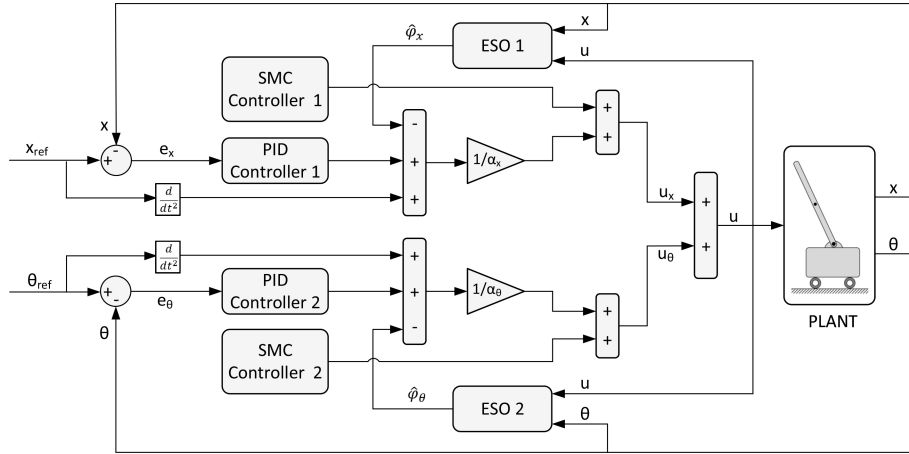


FIGURE 3. iPIDSMC control scheme of the inverted pendulum system.

$$\begin{aligned}
 &= \frac{1}{\alpha_x} \left( \ddot{x}_r(t) - \hat{\varphi}_x(t) - \varphi_{xup} + c_1 \dot{e}_x(t) \right. \\
 &\quad \left. + \kappa_x s_x(t) + \eta_x \operatorname{sgn}(s_x(t)) \right) \\
 &+ \frac{1}{\alpha_\theta} \left( \ddot{\theta}_r(t) - \hat{\varphi}_\theta(t) - \varphi_{\theta up} + c_2 \dot{e}_\theta(t) \right. \\
 &\quad \left. + \kappa_\theta s_\theta(t) + \eta_\theta \operatorname{sgn}(s_\theta(t)) \right) \quad (43)
 \end{aligned}$$

Substituting (41) into (4) and (42) into (5) yields

$$\begin{aligned}
 \ddot{x}(t) + \tilde{\varphi}_x(t) - \varphi_{xup} + c_1 \dot{e}_x(t) \\
 + \kappa_x s_x(t) + \eta_x \operatorname{sgn}(s_x(t)) = 0 \quad (44)
 \end{aligned}$$

$$\begin{aligned}
 \ddot{\theta}(t) + \tilde{\varphi}_\theta(t) - \varphi_{\theta up} + c_2 \dot{e}_\theta(t) \\
 + \kappa_\theta s_\theta(t) + \eta_\theta \operatorname{sgn}(s_\theta(t)) = 0 \quad (45)
 \end{aligned}$$

In order to analyze the stability of the system, Lyapunov function candidate can be selected as

$$V(t) = \frac{1}{2} (s_x^2 + s_\theta^2) \quad (46)$$

From (33), (34), (44) and (45), derivative of the Lyapunov function candidate is written as,

$$\begin{aligned}
 \dot{V}(t) &= s_x \dot{s}_x + s_\theta \dot{s}_\theta \\
 &= s_x (\varphi_{xup} - \tilde{\varphi}_x - \kappa_x - \eta_x \operatorname{sign}(s_x)) \\
 &\quad + s_\theta (\varphi_{\theta up} - \tilde{\varphi}_\theta - \kappa_\theta - \eta_\theta \operatorname{sign}(s_\theta)) \\
 &= -\kappa_x s_x^2 - s_x (\eta_x \operatorname{sign}(s_x) - (\varphi_{xup} - \tilde{\varphi}_x)) \\
 &\quad - \kappa_\theta s_\theta^2 - s_\theta (\eta_\theta \operatorname{sign}(s_\theta) - (\varphi_{\theta up} - \tilde{\varphi}_\theta)) \\
 &\leq -\kappa_x s_x^2 - |s_x| (\eta_x - |\varphi_{xup} - \tilde{\varphi}_x|) \\
 &\quad - \kappa_\theta s_\theta^2 - |s_\theta| (\eta_\theta - |\varphi_{\theta up} - \tilde{\varphi}_\theta|) \quad (47)
 \end{aligned}$$

Therefore, according to boundedness of  $\tilde{\varphi}_x$  and  $\tilde{\varphi}_\theta$ , it is ensured that  $\dot{V}(t) < 0$  in case of  $\eta_x > 2\varphi_{xup}$  and  $\eta_\theta > 2\varphi_{\theta up}$ .

## V. RESULTS AND DISCUSSION

Various simulation studies are carried out to examine the response speed, robustness and disturbance rejection ability of the proposed controller. For a clearer evaluation, control

results of the proposed iPIDSMC controller are compared with the classical PID, iPID and hierarchical sliding mode control (HSMC) results. The parameters of the system used in the simulation studies are,  $m_c = 0.5$  kg,  $m_p = 0.2$  kg,  $L = 0.3$  m. The controller gains of the PID and iPID are optimized by “simplex search” algorithm in Matlab Response Optimizer Toolbox whereas the parameters of the HSMC and the proposed iPIDSMC controller are determined by trial and error method. As a result of the optimization, parameters of the PID and iPID controller are found as  $K_{p1} = 2.2$ ,  $K_{d1} = 2.3$ ,  $K_{i1} = 0.01$ ,  $K_{p2} = 1$ ,  $K_{d2} = 1.1$ ,  $K_{i2} = 0.1$ ,  $\alpha_x = 2.5$ ,  $\alpha_\theta = 33.4$ . The parameters of the iPIDSMC are determined as  $c_1 = 1.5$ ,  $c_2 = 31$ ,  $\kappa_x = 20$ ,  $\kappa_\theta = 20$ ,  $\eta_x = 0.5$ ,  $\eta_\theta = 0.5$  by trial and error method. The upper limits of the disturbances and the observer frequency are selected as,  $\varphi_{xup} = 0.1$ ,  $\varphi_{\theta up} = 0.05$ ,  $\omega_{ESO} = 20$  respectively. All the simulations are started from the vertical upward position where the pendulum was unstable. The initial conditions of the system are  $x = 0$ ,  $\theta = 0^\circ$ ,  $\dot{x} = 0$ ,  $\dot{\theta} = 0$ . In all of the simulation studies, the reference position was taken as 0.5 m step input for the cart and  $0^\circ$  for the pendulum.

Simulation 1: The performances of the controllers are tested under the ideal system conditions without parameter variations or external disturbances and the controller responses are given in Fig. 4. In terms of the response speed, it is clearly seen that the HSMC and the iPIDSMC shows a better performance than the PID and the iPID controllers. For both the cart position and the pendulum angle, the iPIDSMC and the HSMC reached the reference about one second before the PID and iPID controller. Also, no steady-state errors are observed in any of the controller responses.

Simulation 2: The robustness of the controllers against the parameter variations are tested in the second simulation study. Controller responses when the cart and pendulum masses are increased by 100% ( $m_p = 0.4$  kg,  $m_c = 1$  kg) and 200% ( $m_p = 0.8$  kg and  $m_c = 2$  kg) are given in Fig. 5 and Fig. 6 respectively. It is seen that the PID controller is extremely sensitive to parameter variations, shows excessive oscillations in the response at 100% mass increase and

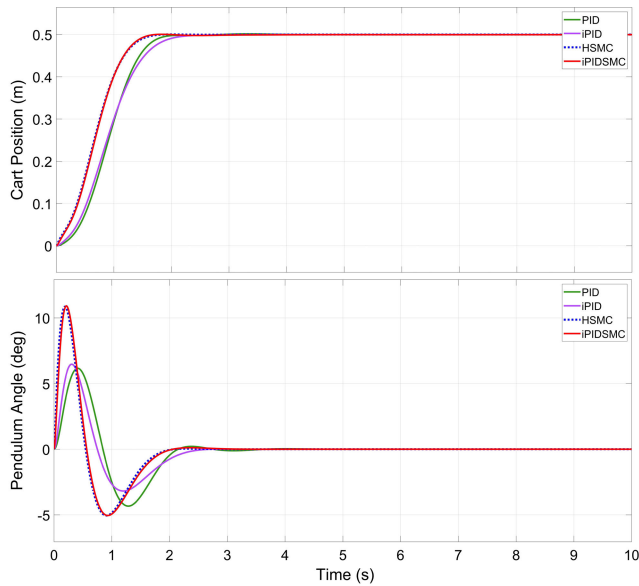


FIGURE 4. Controller responses in the ideal conditions (no parameter changes or external disturbances).

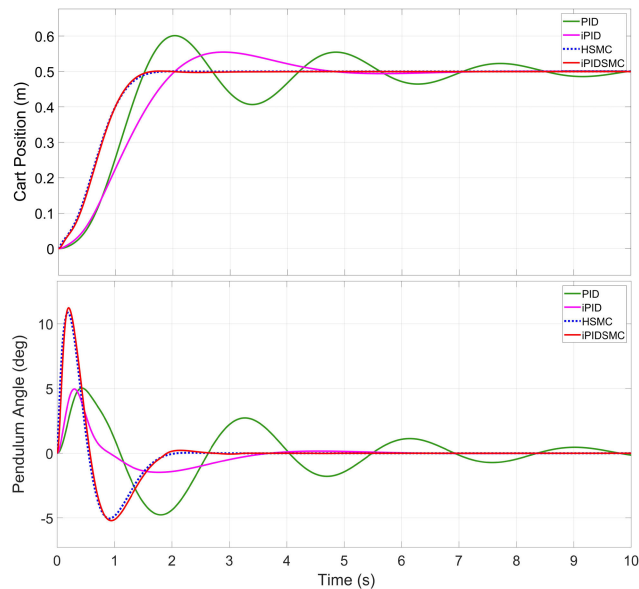


FIGURE 5. Control responses when the cart and pendulum masses are increased by 100%.

becomes unstable at 200% mass increase. Although the iPID controller is less sensitive to parameter variations than the PID controller, there is a significant overshoot in the cart position and some oscillation at the pendulum angle. However, both the iPIDSMC and the HSMC appears to be extremely robust to the parameter variations. Although the cart and the pendulum masses are increased by 200%, no oscillation is observed neither in the cart position nor in the pendulum angle. On the other hand, in both cases, the HSMC appears to be slightly faster than the iPIDSMC.

Simulation 3: The disturbance rejection ability of the controllers against the matched disturbances are tested in the

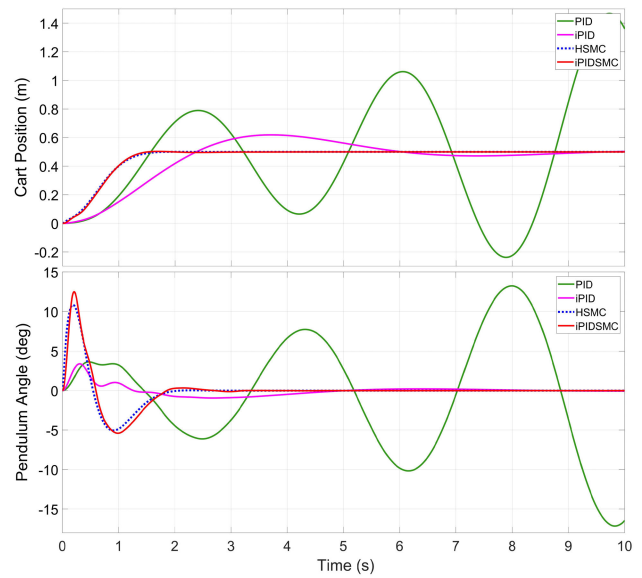


FIGURE 6. Control responses when the cart and pendulum masses are increased by 200%.

third simulation study. First,  $d(t) = 0.1\sin(\pi t)$  sinusoidal disturbance is applied to the system for 10 seconds and then a pulse disturbance with a width of 0.05 and magnitude of 0.2 N was applied to the system at the 5th second. The controller responses are given in Fig. 7 and Fig. 8, respectively. It can be seen from Fig. 7 that the PID control response has a significant amount of oscillation in case of sinusoidal disturbance. Although the iPID controller can suppress the disturbance a bit, there is still a significant amount of oscillation in the response. The iPIDSMC can largely suppress the disturbance except very small oscillations. On the other hand, it can be seen from Fig. 7 that the HSMC can greatly suppress the sinusoidal disturbance and provide an almost smooth response. It can be seen from Fig. 8 that the PID and the iPID responses shows large deviations in case of the pulse disturbance but the iPIDSMC can largely eliminates the disturbance. On the other hand, the best performance is achieved from the HSMC.

Simulation 4: In the fourth simulation study, the disturbance rejection abilities of the controllers are tested against the mismatched disturbance that acts from a different channel than the control input. First,  $d(t) = 0.1\sin(\pi t)$  sinusoidal disturbance and then pulse disturbance with a width of 0.05 and magnitude of 0.2 N is applied to system and the controller responses are given in Fig. 9 and Fig. 10, respectively. It can be seen from Fig. 9 that the PID, iPID and HSMC controllers gave a highly oscillatory response against to sinusoidal disturbance but the iPIDSMC controller largely eliminated the mismatched disturbance and provided an almost smooth response for both the cart position and the pendulum angle. Similar results are obtained for the pulse disturbance as seen from Fig. 10. While the iPIDSMC provides an almost smooth response by greatly suppressing the pulse disturbance, there are large deviations in the PID, iPID and HSMC controllers responses.



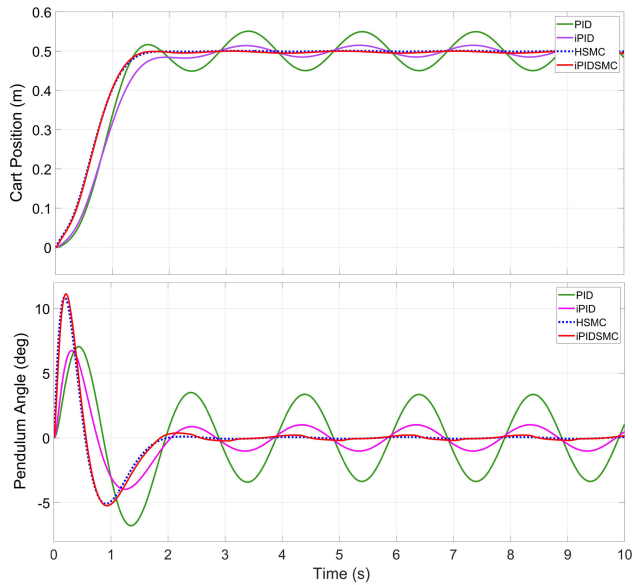


FIGURE 7. Control responses in case of matched sinusoidal disturbance.

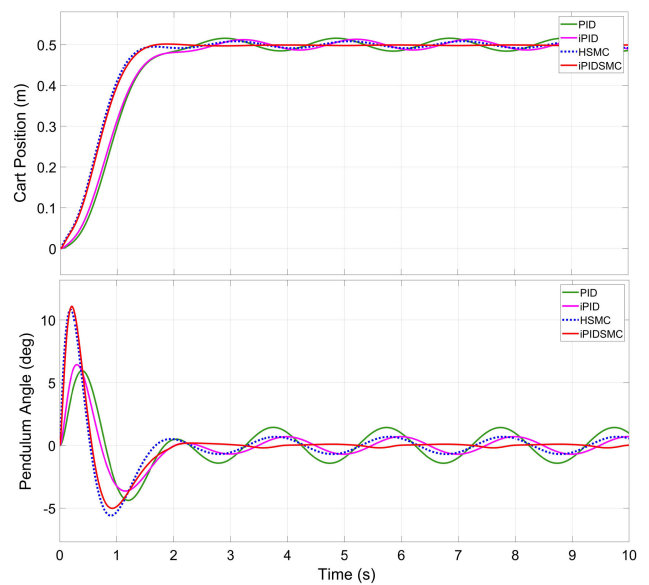


FIGURE 9. Controller responses in case of mismatched sinusoidal disturbance.

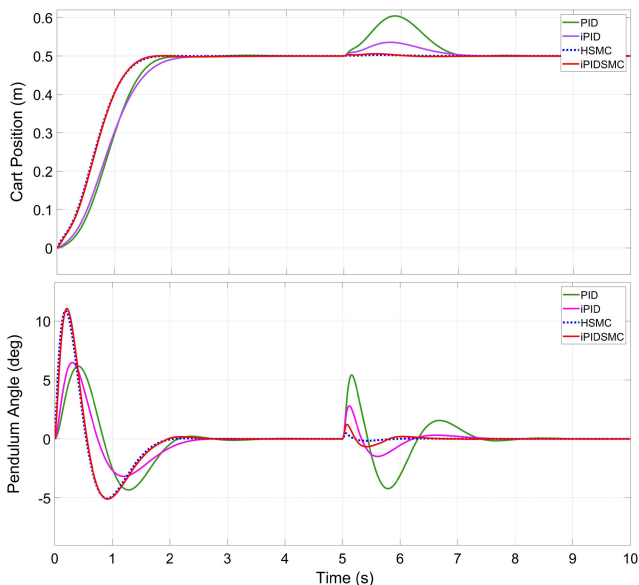


FIGURE 8. Control responses in case of matched pulse disturbance.

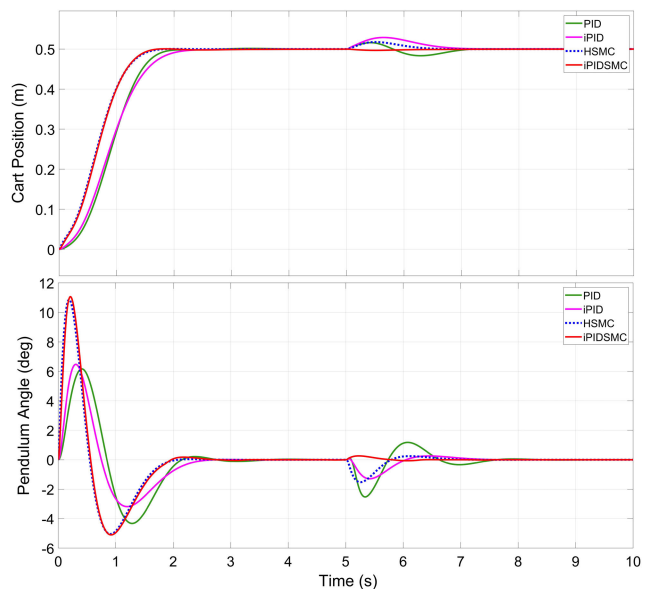
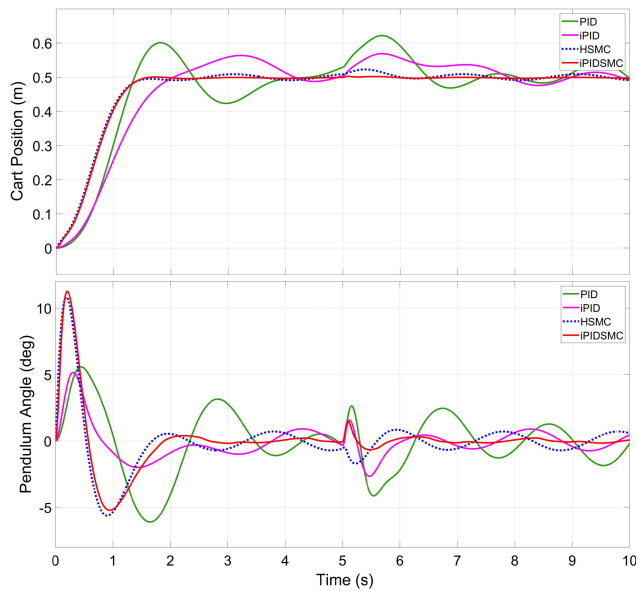


FIGURE 10. Controller responses in case of mismatched pulse disturbance.

Simulation 5: As the final simulation study, all of the matched and unmatched sinusoidal and impact disturbances in the previous simulations are applied to the system at the same time, and in addition, the cart and the pendulum masses are increased by 100%. Control responses and control forces are given comparatively in Fig. 11 and Fig. 12 respectively. This simulation clearly demonstrates the superior success of the proposed iPIDSMC controller in terms of robustness and disturbance rejection ability. As can be seen from Fig. 11, both the PID and iPID controllers give a highly oscillating response to disturbance inputs and mass increase. Although the HSMC controller has somewhat eliminated the effects of disturbances and mass increase, there is still some oscillation in both the cart and pendulum angle response.

On the other hand, the proposed controller gives an almost smooth response by largely eliminating the disturbances and parameter variations.

It can be seen from Fig. 12 that all control forces are within the applicable actuator limits. Furthermore, although both are based on a discontinuous control law, it can be seen that chattering occurs in the HSMC control signal, but the proposed control method is chattering-free. The term chattering describes the phenomenon of finite-frequency, finite-amplitude oscillations appearing in many sliding mode implementations. These oscillations are caused by the high frequency switching of a sliding mode controller exciting unmodeled dynamics in the closed loop [41]. An asymptotic



**FIGURE 11.** Control responses when the cart and pendulum masses are increased by 100% in addition to the total disturbance (sum of the matched and mismatched sinusoidal and pulse disturbances).

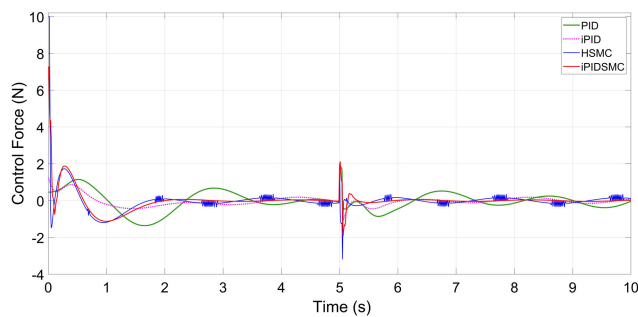


**FIGURE 12.** Control forces in case of increasing the cart and pendulum masses by 100% in addition to the total disturbance (sum of the matched and mismatched sinusoidal and pulse disturbances).

observer in the control loop can eliminate the chattering despite discontinuous control laws. The key idea is to generate an ideal sliding mode in the observer loop rather than in the main control loop, and this is possible since the observer loop does not contain any unmodeled dynamics [41]. The results indicate that the proposed control method successfully eliminates all unmodeled dynamics, resulting in an ideal sliding mode that ensures that the control signal is chattering-free.

## VI. CONCLUSION

External disturbances and parameter variations often encountered in practical applications always cause adverse effects to the stability and performance of control systems. In this study, we proposed a model-free control scheme based on iPID and SMC for the systems with parameter variations and external disturbances. The proposed control scheme is basically built on the iPID control theory. Since the effectiveness of the iPID control depends on the success of the

observer, the SMC controller was added to the control scheme in order to minimize the estimation errors and guarantee that the tracking errors converge to zero asymptotically. Stability of the proposed control scheme has been proven by Lyapunov stability analysis. An inverted pendulum - cart system was selected to investigate the performance of the proposed controller because, in addition to underactuated, unstable, and non-linear properties, unmodeled dynamics, load variations, and external disturbances make the systems much more difficult to control. The proposed control scheme has been tested in terms of response speed, robustness and disturbance rejection ability with different simulation studies, including parameter variations and disturbances and its performance has been compared with the conventional PID, HSMC and iPID controllers. Simulation results show that the performance of the proposed controller is much better than the other controllers. Also it is seen that the proposed controller is totally insensitive to parameter variations as well as it has a superior disturbance rejection ability against the matched and mismatched disturbances. Furthermore, the control signal of the proposed method is chattering-free, even though it is based on an SMC using discontinuous control action. On the other hand, although the proposed control method is based on a simple theory, it has a large number of parameters that must be adjusted to achieve the proper control effect. The biggest challenge in this study was the proper determination of control parameters by trial and error method. In future works, it is aimed to systematically determine the controller parameters by using genetic algorithm, particle swarm optimization, bee algorithm or similar optimization methods.

## REFERENCES

- [1] L. B. Prasad, B. Tyagi, and H. O. Gupta, "Optimal control of nonlinear inverted pendulum system using PID controller and LQR: Performance analysis without and with disturbance input," *Int. J. Autom. Comput.*, vol. 11, no. 6, pp. 667–670, Dec. 2014, doi: [10.1007/s11633-014-0818-1](https://doi.org/10.1007/s11633-014-0818-1).
- [2] R. Shalaby, M. El-Hossainy, and B. Abo-Zalam, "Fractional order modeling and control for under-actuated inverted pendulum," *Commun. Nonlinear Sci. Numer. Simul.*, vol. 74, pp. 97–121, Jul. 2019, doi: [10.1016/j.cnsns.2019.02.023](https://doi.org/10.1016/j.cnsns.2019.02.023).
- [3] J. Pongfai, C. Angeli, P. Shi, X. Su, and W. Assawinchaichote, "Optimal PID controller autotuning design for MIMO nonlinear systems based on the adaptive SLP algorithm," *Int. J. Control. Autom. Syst.*, vol. 19, no. 1, pp. 392–403, Jan. 2021, doi: [10.1007/s12555-019-0680-6](https://doi.org/10.1007/s12555-019-0680-6).
- [4] Ü. Önen, A. Çakan, and I. İlhan, "Performance comparison of optimization algorithms in LQR controller design for a nonlinear system," *TURKISH J. Electr. Eng. Comput. Sci.*, vol. 27, no. 3, pp. 1938–1953, May 2019, doi: [10.3906/elk-1808-51](https://doi.org/10.3906/elk-1808-51).
- [5] M. El-Bardini and A. M. El-Nagar, "Interval type-2 fuzzy PID controller for uncertain nonlinear inverted pendulum system," *ISA Trans.*, vol. 53, pp. 732–743, May 2014, doi: [10.1016/j.isatra.2014.02.007](https://doi.org/10.1016/j.isatra.2014.02.007).
- [6] M. Fallahi and S. Azadi, "Adaptive control of an inverted pendulum using adaptive PID neural network," in *Proc. Int. Conf. Signal Process. Syst.*, Singapore, 2009, pp. 589–593, doi: [10.1109/ICSPS.2009.110](https://doi.org/10.1109/ICSPS.2009.110).
- [7] V. Veselý and I. Adrian, "Gain-scheduled PID controller design," *J. Process Control*, vol. 23, no. 8, pp. 1141–1148, 2013, doi: [10.1016/j.jprocont.2013.07.002](https://doi.org/10.1016/j.jprocont.2013.07.002).
- [8] L. Messikh, E. H. Guechi, and M. L. Benloucif, "Critically damped stabilization of inverted-pendulum systems using continuous-time cascade linear model predictive control," *J. Franklin Inst.*, vol. 354, no. 16, pp. 7241–7265, Nov. 2017, doi: [10.1016/j.franklin.2017.08.039](https://doi.org/10.1016/j.franklin.2017.08.039).

- [9] M. Yue, C. An, and J.-Z. Sun, "An efficient model predictive control for trajectory tracking of wheeled inverted pendulum vehicles with various physical constraints," *Int. J. Control, Autom. Syst.*, vol. 16, no. 1, pp. 265–274, Feb. 2018, doi: [10.1007/s12555-016-0393-z](https://doi.org/10.1007/s12555-016-0393-z).
- [10] X. Tian, H. Peng, F. Zhou, and X. Peng, "RBF-ARX model-based fast robust MPC approach to an inverted pendulum," *ISA Trans.*, vol. 93, pp. 255–267, Oct. 2019, doi: [10.1016/j.isatra.2019.02.035](https://doi.org/10.1016/j.isatra.2019.02.035).
- [11] M. S. Mahmoud and M. T. Nasir, "Robust control design of wheeled inverted pendulum assistant robot," *IEEE/CAA J. Autom. Sinica*, vol. 4, no. 4, pp. 628–638, Sep. 2017, doi: [10.1109/JAS.2017.7510613](https://doi.org/10.1109/JAS.2017.7510613).
- [12] S. Jung and S. Su Kim, "Control experiment of a wheel-driven mobile inverted pendulum using neural network," *IEEE Trans. Control Syst. Technol.*, vol. 16, no. 2, pp. 297–303, Mar. 2008, doi: [10.1109/TCST.2007.903396](https://doi.org/10.1109/TCST.2007.903396).
- [13] S. Yang, Z. Li, R. Cui, and B. Xu, "Neural network-based motion control of an underactuated wheeled inverted pendulum model," *IEEE Trans. Neural Netw. Learn. Syst.*, vol. 25, no. 11, pp. 2004–2016, Nov. 2014, doi: [10.1109/TNNLS.2014.2302475](https://doi.org/10.1109/TNNLS.2014.2302475).
- [14] A. Unluturk and O. Aydogdu, "Machine learning based self-balancing and motion control of the underactuated mobile inverted pendulum with variable load," *IEEE Access*, vol. 10, pp. 104706–104718, 2022, doi: [10.1109/ACCESS.2022.3210540](https://doi.org/10.1109/ACCESS.2022.3210540).
- [15] Z. B. Hazem, M. J. Fotuhi, and Z. Bingül, "Anti-swing radial basis neuro-fuzzy linear quadratic regulator control of double link rotary pendulum," *Proc. Inst. Mech. Eng., I, J. Syst. Control Eng.*, vol. 236, no. 3, pp. 531–545, Mar. 2022, doi: [10.1177/09596518211046452](https://doi.org/10.1177/09596518211046452).
- [16] Y. Shao and J. Li, "Modeling and switching tracking control for a class of cart-pendulum systems driven by DC motor," *IEEE Access*, vol. 8, pp. 44858–44866, 2020, doi: [10.1109/ACCESS.2020.2978269](https://doi.org/10.1109/ACCESS.2020.2978269).
- [17] F. Adıgüzel and Y. Yalçın, "Backstepping control for a class of underactuated nonlinear mechanical systems with a novel coordinate transformation in the discrete-time setting," *Proc. Inst. Mech. Eng., I, J. Syst. Control Eng.*, vol. 236, no. 6, pp. 1211–1223, Jul. 2022, doi: [10.1177/09596518221079940](https://doi.org/10.1177/09596518221079940).
- [18] R. Rascon, D. I. Rosas, and J. C. Rodríguez-Quirón, "Robust continuous control for a class of mechanical systems based on nonsingular terminal sliding mode," *IEEE Access*, vol. 8, pp. 19297–19305, 2020, doi: [10.1109/ACCESS.2020.2965596](https://doi.org/10.1109/ACCESS.2020.2965596).
- [19] H. Dong, X. Yang, H. Gao, and X. Yu, "Practical terminal sliding-mode control and its applications in servo systems," *IEEE Trans. Ind. Electron.*, vol. 70, no. 1, pp. 752–761, Jan. 2023, doi: [10.1109/TIE.2022.3152018](https://doi.org/10.1109/TIE.2022.3152018).
- [20] F. F. M. El-Sousy, K. A. Alattas, O. Mofid, S. Mobayen, and A. Fekih, "Robust adaptive super-twisting sliding mode stability control of underactuated rotational inverted pendulum with experimental validation," *IEEE Access*, vol. 10, pp. 100857–100866, 2022, doi: [10.1109/ACCESS.2022.3208412](https://doi.org/10.1109/ACCESS.2022.3208412).
- [21] S. Hwang and H. S. Kim, "Extended disturbance observer-based integral sliding mode control for nonlinear system via T-S fuzzy model," *IEEE Access*, vol. 8, pp. 116090–116105, 2020, doi: [10.1109/ACCESS.2020.3004241](https://doi.org/10.1109/ACCESS.2020.3004241).
- [22] Z. Ma, Z. Liu, P. Huang, and Z. Kuang, "Adaptive fractional-order sliding mode control for admittance-based telerobotic system with optimized order and force estimation," *IEEE Trans. Ind. Electron.*, vol. 69, no. 5, pp. 5165–5174, May 2022, doi: [10.1109/TIE.2021.3078385](https://doi.org/10.1109/TIE.2021.3078385).
- [23] J. Hu, H. Zhang, H. Liu, and X. Yu, "A survey on sliding mode control for networked control systems," *Int. J. Syst. Sci.*, vol. 52, no. 6, pp. 1129–1147, Apr. 2021, doi: [10.1080/00207721.2021.1885082](https://doi.org/10.1080/00207721.2021.1885082).
- [24] M. Ramirez-Neria, H. Sira-Ramirez, R. Garrido-Moctezuma, A. Luviano-Juárez, and Z. Gao, "Active disturbance rejection control for reference trajectory tracking tasks in the pendubot system," *IEEE Access*, vol. 9, pp. 102663–102670, 2021, doi: [10.1109/ACCESS.2021.3096138](https://doi.org/10.1109/ACCESS.2021.3096138).
- [25] Y. Huang and W. Xue, "Active disturbance rejection control: Methodology and theoretical analysis," *ISA Trans.*, vol. 53, no. 4, pp. 963–976, Apr. 2014, doi: [10.1016/j.isatra.2014.03.003](https://doi.org/10.1016/j.isatra.2014.03.003).
- [26] H. Pan and W. Sun, "Nonlinear output feedback finite-time control for vehicle active suspension systems," *IEEE Trans. Ind. Informat.*, vol. 15, no. 4, pp. 2073–2082, Apr. 2019, doi: [10.1109/TII.2018.2866518](https://doi.org/10.1109/TII.2018.2866518).
- [27] F. Li, F. Yang, and Q. Li, "Event-triggered consensus control for nonlinear multiagent systems with unmeasured state variables," *IEEE Access*, vol. 10, pp. 77030–77038, 2022, doi: [10.1109/ACCESS.2022.3192611](https://doi.org/10.1109/ACCESS.2022.3192611).
- [28] H. Pan, D. Zhang, W. Sun, and X. Yu, "Event-triggered adaptive asymptotic tracking control of uncertain MIMO nonlinear systems with actuator faults," *IEEE Trans. Cybern.*, vol. 52, no. 9, pp. 8655–8667, Sep. 2022, doi: [10.1109/TCYB.2021.3061888](https://doi.org/10.1109/TCYB.2021.3061888).
- [29] M. Fliess and C. Join, "Intelligent PID controllers," in *Proc. 16th Medit. Conf. Control Autom.*, Ajaccio, France, Jun. 2008, pp. 326–331, doi: [10.1109/MED.2008.4601995](https://doi.org/10.1109/MED.2008.4601995).
- [30] M. Fliess, "Model-free control and intelligent PID controllers: Towards a possible trivialization of nonlinear control?" *IFAC Proc. Volumes*, vol. 42, no. 10, pp. 1531–1550, 2009, doi: [10.3182/20090706-3-FR-2004.00256](https://doi.org/10.3182/20090706-3-FR-2004.00256).
- [31] M. Fliess and C. Join, "Model-free control," *Int. J. Control*, vol. 86, no. 12, pp. 2228–2252, Jul. 2013, doi: [10.1080/00207179.2013.810345](https://doi.org/10.1080/00207179.2013.810345).
- [32] S. Andary, A. Chemori, M. Benoit, and J. Sallantin, "A dual model-free control of underactuated mechanical systems, application to the inertia wheel inverted pendulum," in *Proc. Amer. Control Conf. (ACC)*, Montreal, QC, Canada, Jun. 2012, pp. 1029–1034, doi: [10.1109/ACC.2012.6315492](https://doi.org/10.1109/ACC.2012.6315492).
- [33] C.-Y. Yu and J.-L. Wu, "Intelligent PID control for two-wheeled inverted pendulums," in *Proc. Int. Conf. Syst. Sci. Eng. (ICSSE)*, Puli, Taiwan, Jul. 2016, pp. 1–4, doi: [10.1109/ICSSE.2016.7551542](https://doi.org/10.1109/ICSSE.2016.7551542).
- [34] İ. Yiğit, "Model free sliding mode stabilizing control of a real rotary inverted pendulum," *J. Vibrot. Control*, vol. 23, no. 10, pp. 1645–1662, Aug. 2015, doi: [10.1177/1077546315598031](https://doi.org/10.1177/1077546315598031).
- [35] J. Huang, T. Zhang, Y. Fan, and J.-Q. Sun, "Control of rotary inverted pendulum using model-free backstepping technique," *IEEE Access*, vol. 7, pp. 96965–96973, 2019, doi: [10.1109/ACCESS.2019.2930220](https://doi.org/10.1109/ACCESS.2019.2930220).
- [36] R. Zarei and S. Khorashadizadeh, "Direct adaptive model-free control of a class of uncertain nonlinear systems using legendre polynomials," *Trans. Inst. Meas. Control*, vol. 41, no. 11, pp. 3081–3091, Jan. 2019, doi: [10.1177/0142331218821408](https://doi.org/10.1177/0142331218821408).
- [37] A. Ghio and O. E. Ramos, "Q-learning-based model-free swing up control of an inverted pendulum," in *Proc. IEEE 26th Int. Conf. Electron., Electr. Eng. Comput. (INTERCON)*, Lima, Peru, Aug. 2019, pp. 1–4, doi: [10.1109/INTERCON.2019.8853619](https://doi.org/10.1109/INTERCON.2019.8853619).
- [38] O. Tutsoy and D. E. Barkana, "Model free adaptive control of the under-actuated robot manipulator with the chaotic dynamics," *ISA Trans.*, vol. 118, pp. 106–111, Dec. 2021, doi: [10.1016/j.isatra.2021.02.006](https://doi.org/10.1016/j.isatra.2021.02.006).
- [39] C.-H. Chiu, Y.-W. Lin, and C.-H. Lin, "Real-time control of a wheeled inverted pendulum based on an intelligent model free controller," *Mechatronics*, vol. 21, no. 3, pp. 523–533, Apr. 2011, doi: [10.1016/j.mechatronics.2011.01.010](https://doi.org/10.1016/j.mechatronics.2011.01.010).
- [40] L. Zhang, Z. Li, and C. Yang, "Adaptive neural network based variable stiffness control of uncertain robotic systems using disturbance observer," *IEEE Trans. Ind. Electron.*, vol. 64, no. 3, pp. 2236–2245, Mar. 2017, doi: [10.1109/TIE.2016.2624260](https://doi.org/10.1109/TIE.2016.2624260).
- [41] V. Utkin, J. Guldner, and J. Shi, *Sliding Mode Control in Electro-Mechanical Systems*, 2nd ed. Boca Raton, FL, USA: CRC Press, 2017, doi: [10.1201/9781420065619](https://doi.org/10.1201/9781420065619).



**ÜMIT ÖNEN** received the B.S., M.S., and Ph.D. degrees in mechanical engineering from Selçuk University, Konya, Turkey, in 2001, 2004, and 2011, respectively. From 2001 to 2011, he was a Research Assistant at the Mechanical Engineering Department, Selçuk University. Since 2011, he has been an Assistant Professor with the Mechatronics Engineering Department, Necmettin Erbakan University, Konya. His research interests include multi-body dynamics, robotics, exoskeleton systems, linear control theory, and robust control.

• • •